

The elastic microstructures of inkjet printed polydimethylsiloxane as the patterned dielectric layer for pressure sensors

Yongyi Peng, Shugang Xiao, Junliang Yang, Jian Lin, Wei Yuan, Weibing Gu, Xinzhou Wu, and Zheng Cui

Citation: *Appl. Phys. Lett.* **110**, 261904 (2017); doi: 10.1063/1.4990528

View online: <http://dx.doi.org/10.1063/1.4990528>

View Table of Contents: <http://aip.scitation.org/toc/apl/110/26>

Published by the [American Institute of Physics](#)

AIP | Applied Physics
Letters

Save your money for your research.
It's now **FREE** to publish with us -
no page, color or publication charges apply.

If your article has the
potential to shape the future of
applied physics, it BELONGS in
Applied Physics Letters

The elastic microstructures of inkjet printed polydimethylsiloxane as the patterned dielectric layer for pressure sensors

Yongyi Peng,¹ Shugang Xiao,^{1,2} Junliang Yang,^{1,a)} Jian Lin,^{2,b)} Wei Yuan,² Weibing Gu,² Xinzhou Wu,² and Zheng Cui²

¹Hunan Key Laboratory for Super-microstructure and Ultrafast Process, School of Physics and Electronics, Central South University, Changsha 410083, China

²Printable Electronics Research Centre, Suzhou Institute of Nano-tech and Nano-Bionics, Chinese Academy of Sciences, No. 398 Ruoshui Road, SEID, Suzhou Industrial Park, Suzhou, Jiangsu Province 215123, People's Republic of China

(Received 27 March 2017; accepted 15 June 2017; published online 29 June 2017)

A direct inkjet printing process was developed to fabricate patterned elastic microstructures for pressure sensors using n-butyl acetate diluted polymethylsiloxane (PDMS). The diluted PDMS precursor mixture with a cross-linker exhibited a controllable viscosity below 14 cP in 48 h at 25 °C, and the PDMS film had lower elastic modulus and hardness values than the non-diluted PDMS precursor after curing. The capacitor using the printed PDMS film as the microstructured dielectric layer showed a very high pressure sensitivity of up to 10.4 kPa⁻¹ under the pressure below 70 Pa, and the pressure sensitivity would be dramatically decreased to 0.043–0.052 kPa⁻¹ under the pressure between 2 and 8 kPa. Furthermore, the triboelectric sensors could be structured with an inkjet printed PDMS film and controllably generate the voltage signals up to 1.23 V without any amplification. The results suggest that mechanical properties and patterned elastic microstructures play the key roles in PDMS-based sensor devices, and the PDMS dielectric layer with controlled mechanical properties and microstructures fabricated via directly inkjet printing opens up the applications of the PDMS and its composites in functional devices. *Published by AIP Publishing.*

[<http://dx.doi.org/10.1063/1.4990528>]

Polydimethylsiloxane (PDMS) is a typical silicone elastomer with excellent properties such as stretchability, chemical/physiological/thermal stability, low modulus, and optical transparency, as well as low cost and ease of fabrication. It has been widely used in microfluidics,¹ soft lithography,² analytical chemistry,³ electronics,⁴ medical devices,⁵ and polymeric optics.⁶ Over the past few years, PDMS and its composites were reported in the application of sensors^{7,8} and energy harvests.^{9,10} The microstructured PDMS film has been proven to be the key element for high sensitivity and fast response time in capacitive,¹¹ triboelectric,⁹ and piezoresistive¹² pressure sensors.

Comparing with the microstructures fabricated by replica molding^{11,12} or other potential large-area printing/coating techniques,^{13–15} inkjet printing is a low-cost and convenient non-contact method for depositing the materials with customized patterns.¹⁶ However, it is normally impossible to make the PDMS precursor to be jetted out by the piezoelectrically driven inkjet printhead due to the high viscosity and continuous cross-linking reaction. Although it could be jetted out by an injector with a volume ranging from 10 μl to 100 μl,¹⁷ it is still very difficult to produce pL-scaled droplets.

Diluting the PDMS precursor with functional solvents is a simple and effective method to decrease the viscosity. It was reported that a 70 nm PDMS film could be achieved by spin-coating the hexane diluted precursor.¹⁸ Furthermore, the properly diluted mixture could be processed by using the spraying technique.¹⁹ In this letter, the PDMS precursor was

diluted with a good solvent and its direct inkjet printed patterned film with pL-scaled droplets was used as the microlens or microstructured dielectric layer for pressure sensors.

To eliminate the nozzle clogging, high boiling n-butyl acetate was chosen as the diluting solvent to reduce the ink evaporation during the printing process. The PDMS precursor mixture with a cross-linker (Dow Corning Sylgard 184, the weight ratio of the base to the cross-linker was 10:1) was diluted with a volume ratio of 1:3 (PDMS to solvent). The diluted mixture by stirring for 10 min at least could be printed by a MicroFab jetlab II inkjet printer with a 50 μm diameter printhead. The PDMS was printed directly on indium tin oxide (ITO) coated glass, which was cleaned by sonication in acetone, deionized water, and isopropanol, respectively, followed by the curing process at 115 °C for 30 min. The viscosity was measured by using a digital viscometer (Nirun, SNB-1), and the sample surface was measured by using a Dektak XT stylus profiler. The nanoindentation was performed by using an Agilent Nanoindenter G200.

The schematic diagram of the inkjet printing PDMS pattern and the scanning electron microscopy (SEM) image of printed droplets are shown in Figs. 1(a) and 1(b), respectively. A single cured PDMS droplet printed on the ITO/glass surface has a very flat spherical segment shape (base outer diameter, 160 μm; height, 1.6 μm) with a volume of about 16 pL [Fig. 1(c)]. The inset in Fig. 1(c) depicts that the images of the luminous filament can be observed from printed PDMS droplets as a microlens array. Furthermore, PDMS can be printed to form any patterns directly on a flexible polyethylene terephthalate (PET) film, as shown in Fig. 1(d).

a) junliang.yang@csu.edu.cn

b) jin2010@sinano.ac.cn

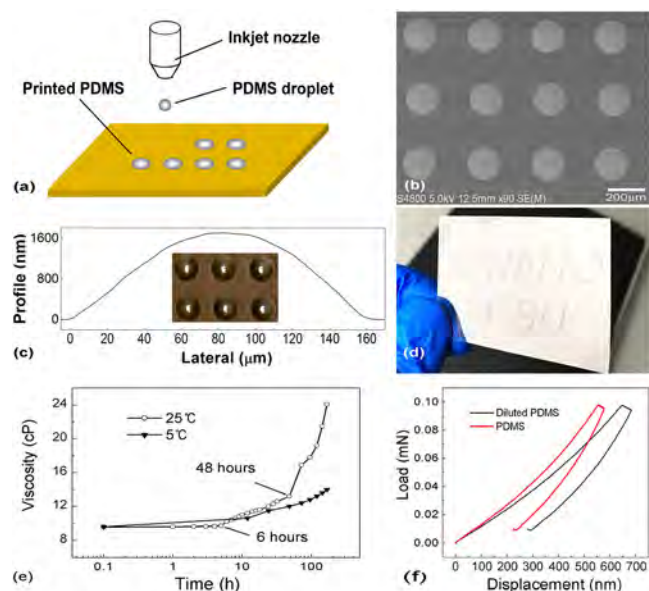


FIG. 1. (a) Schematic diagram of the inkjet printing PDMS microstructure. (b) SEM image of the printed PDMS droplet array. (c) The surface profile of a cured droplet on a substrate. The inset shows the images of the luminous filament observed from printed PDMS droplets. (d) Inkjet printed PDMS with designed patterns on the PET substrate. (e) The viscosity stability of the diluted PDMS mixture at temperatures of 25 and 5 °C. (f) The load-displacement curves of PDMS samples.

A remarkable advantage of the diluted PDMS mixture in this work is that the viscosity can be decreased to less than 10 cP, and it shows little change in a long time. It is well known that, due to the continuous cross-linking reaction, the non-diluted PDMS precursor mixture with a cross-linker should be used as soon as possible because the viscosity increases quickly. On the other hand, Fig. 1(e) displays the viscosity variation of the diluted PDMS mixture at the typical temperatures of 25 and 5 °C. It can be found that the viscosity can be kept below 10 cP in 6 h and below 14 cP in 48 h at 25 °C. If the temperature is decreased to 5 °C, the viscosity of the diluted mixture can be kept less than 14 cP in a week. Considering the rate of the cross-linking reaction reported as a complex function of the precursor's concentration according to the curing kinetics,²⁰ the lower concentration of the diluted PDMS precursor should play a key role in these experimental results. There should be much slower cross-linking reactions between the diluted PDMS precursor and the cross-linker because of the decreased concentration, which can make the curing process much longer. Thanks to the lower concentration and the slow cross-linking rate of the diluted PDMS precursor, the viscosity of PDMS was kept suitable for inkjet printing in a quite long time.

The mechanical properties of the cross-linked PDMS film fabricated via spin-coating using the PDMS precursor with and without diluting were measured as well. Two spin-coated PDMS samples (a thickness of 2.5 μm and the same curing condition as printed PDMS) with and without solvent dilution were studied by the nanoindentation measurement using the Oliver and Pharr method.²¹ The load-displacement curves demonstrate that the diluted PDMS sample has more displacement at the same load during the measurement [Fig. 1(f)], which means that it has lower elastic modulus and hardness. The elastic modulus and hardness of the PDMS

film with the diluted precursor at the max load are calculated to be 105 and 19 MPa, respectively, while the values of the PDMS film with the undiluted precursor are 146 and 27 MPa, respectively. The lower elastic modulus and hardness of diluted PDMS can be explained by the lower concentration before the solvent evaporated during the curing process. The cross-linking reaction of diluted PDMS should be slower than that of the undiluted precursor because of the decreased concentration according to the kinetics.²⁰ As a result, the cross-linking degree of diluted PDMS is lower than that of undiluted samples with the same curing process, which makes diluted PDMS to have the softer mechanical properties. On the other hand, both PDMS films have larger elastic modulus and hardness than the reported results because of the thinner thickness and higher curing temperature.^{22,23}

A series of 10 × 10 mm thin-film capacitors using printed PDMS patterned microstructures as the dielectric layer were fabricated for measuring the capacitance variation under pressures [Fig. 2(a)]. The PDMS was printed with different dot-spacings of 500, 353, 250, and 177 μm, and the corresponding devices were marked as devices P₅₀₀, P₃₅₃, P₂₅₀, and P₁₇₇, respectively. For comparison, a spin-coated undiluted PDMS film using the maximum spin-coating speed on ITO/glass (2.5 μm thickness and the same curing conditions as printed PDMS) was also fabricated and labeled as device S. In order to make sure that there is the good contact between the PDMS and the top ITO surface, a piece of ITO/glass (0.3 g, corresponds to 29.4 Pa) was laminated onto the PDMS microstructures as the top electrode and was set as the “zero-weight”. The capacitance was measured by using a IM3533-1LCR Meter (Hioki Company, Japan).

To understand the overall capacitance changes of different devices, the relative change in the measured capacitance ($\Delta C/C_0$) versus logarithmic pressure is displayed in Fig. 2(b), where C_0 and ΔC denote the initial capacitance and the change in capacitance with applied pressure, respectively. It can be found that the $\Delta C/C_0$ values are in the order of

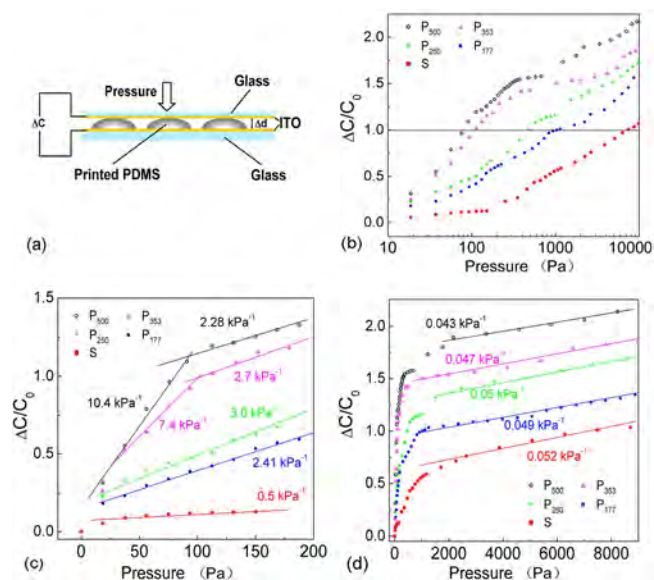


FIG. 2. (a) Schematic of capacitors using printed or spin-coated PDMS as the dielectric layer. (b)–(d) The capacitance change in the pressure range of logarithmic 0–10 kPa, 0–200 Pa, and 2–8 kPa, respectively.

TABLE I. Device performances with different PDMS layers, the curves of which are shown in Figs. 2 and 4.

Device	PDMS coverage (%)	Pressure at $\Delta C/C=1$ (Pa)	Selected calculated sensitivity (kPa^{-1})	Triboelectric output peak voltage (V)
P ₅₀₀	8.0	79.9	10.4/2.28/0.043	0.55
P ₃₅₃	15.68	111.6	7.4/2.7/0.047	0.64
P ₂₅₀	32.0	474.7	3.0/0.05	1.23
P ₁₇₇	62.7	1024.8	2.41/0.049	1.05
S	100	7000	0.5/0.052	0.61

decreasing as $P_{500} > P_{353} > P_{250} > P_{177} > S$ under all the applied pressures. To evaluate different capacitance change rates, the pressures of various devices at $\Delta C/C = 1$ ($C = 2 C_0$) are marked in the figure, the values of which are summarized in Table I. The figure also shows that all the $\Delta C/C_0$ values have much higher increasing speeds in the range of low pressure than those under higher pressure.

The detailed characteristics of $\Delta C/C_0$ under various pressures are shown in Fig. 2(c) (0–200 Pa) and Fig. 2(d) (2–8 kPa). Several representatively calculated pressure sensitivities (defined as the slope of $\Delta C/C_0$ versus applied pressure) are listed in Table I. It can be found that the device P₅₀₀ has a pressure sensitivity as high as 10.4 kPa^{-1} in a pressure range of 0–70 Pa, but it decreases to 2.28 kPa^{-1} in 70–200 Pa. Similarly, the pressure sensitivity of device P₃₅₃ also drops from 7.4 kPa^{-1} (0–70 Pa) to 2.7 kPa^{-1} (70–200 Pa). Different from these two capacitors, the pressure sensitivities of devices P₂₅₀ and P₁₇₇ show the lower values without obvious change in the range of 0–200 Pa, while device S has the lowest value down to 0.5 kPa^{-1} in this pressure range. On the other hand, all the devices have quite similar sensitivity values that are between 0.047 and 0.52 kPa^{-1} in the pressure range of 2–8 kPa.

The rapid change in pressure sensitivity should be attributed to the printed thin PDMS microstructures with low distribution density. According to the surface profiles of PDMS layers [Fig. 3(a)] and the schematic diagram of the capacitor under different pressures [Fig. 3(b)], the printed flat PDMS spherical segment droplets can be pressed into a low circular

cylinder shape under a relatively low pressure, the capacitance of which will increase quickly. At the same time, the dielectric constant of the PDMS-air composited layer also increased when the PDMS ($\epsilon = 3.0$) displaced the volume of air ($\epsilon = 1.0$). It can be calculated that the printed PDMS coverage ratio of devices P₅₀₀ and P₃₅₃ on the bottom ITO surface is 8% and 15.68%, respectively (Table I), which makes them have lower modulus and are more sensitive to small pressure during this process. On the other hand, device S shows much poorer sensitivity in the low pressure range because of the smooth surface and 100% coverage. However, the elastic modulus will dramatically increase if the PDMS layer (both with/without patterned microstructure) is further compressed under a higher pressure, which should be the main reason for the rapid decrease in pressure sensitivity to 0.043 – 0.052 kPa^{-1} in the range of 2–8 kPa. It was reported that the PDMS layer's mechanical strength can be reinforced by the rigid substrate,¹⁷ which may also play a key role in the sensitivity decrease and homoplasia under high pressure.

The patterned microstructured PDMS on the ITO/glass surface was also reported as the active layer for self-powered triboelectric sensors with PET films due to the charge generation and separation between PDMS and PET.⁹ For verifying the triboelectric effects of inkjet printed PDMS microstructures, a series of triboelectric sensors were fabricated with the ITO/PET film covered on the printed and spin-coated PDMS layers (P₅₀₀, P₃₅₃, P₂₅₀, P₁₇₇, and S) with the PET side contacting the PDMS. Figure 4(a) presents the schematic diagram

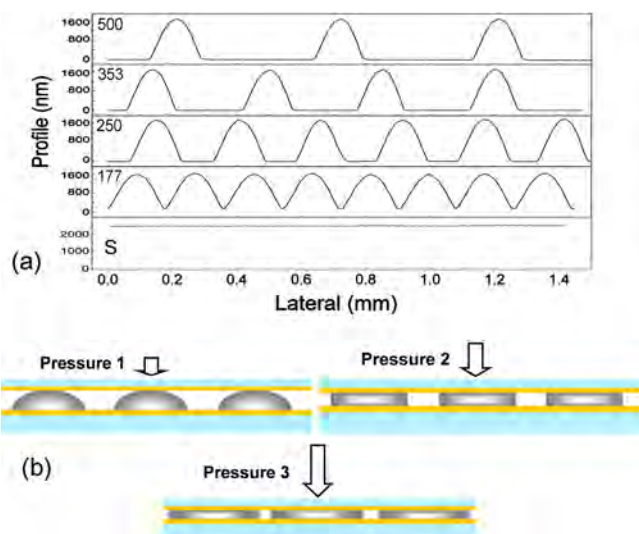


FIG. 3. (a) Surface profiles of the printed PDMS film with different printing dot-spacings and the spin-coated PDMS film. (b) Schematic diagram of the capacitor under different pressures: Pressure 1 < Pressure 2 < Pressure 3.

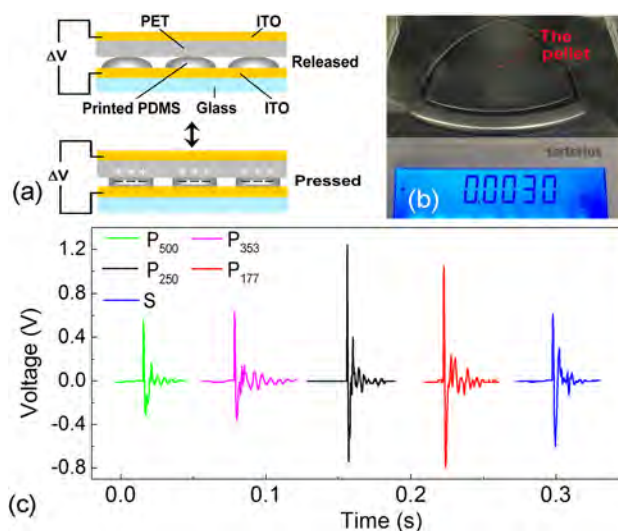


FIG. 4. (a) The schematic structure of the self-powered triboelectric sensor with the printed PDMS dielectric layer. (b) The pellet used for test. (c) Different output voltages for self-power triboelectric sensors with printed and spin-coated PDMS layers.

of the triboelectric sensor and its test method. A small Al-foil pellet [3 mg, about 0.294 Pa in pressure, Fig. 4(b)] is utilized to induce applied force upon the device. The comparison of the output voltages can be found in Fig. 4(c), showing that there were different scales of pulses measured with obvious damped vibrations after the pellet hit the PET film. The device P₂₅₀ produces the best peak voltage up to 1.23 V without any amplification, while the spin-coated device S with the flat surface only shows an output signal of 0.61 V peak voltage. The better performance of P₂₅₀ is attributed to the microstructured PDMS, which has larger effective triboelectric effects during the pressing process, and the triboelectric charges are more easily separated when the device released. The peak voltage of device P₁₇₇ decreases to 1.05 V because of a shorter peak-to-valley PDMS distance than P₂₅₀. On the other hand, the triboelectric charges generated by devices P₅₀₀ and P₃₅₃ are much less than those generated P₂₅₀ due to the lower PDMS coverage (Table I), leading to the peak of the output signal as low as 0.55 V and 0.64 V, respectively. The above results suggest that the triboelectric sensor with good performance should result from the balance between the PDMS coverage and the triboelectric effect.

In summary, the PDMS precursor diluted by n-butyl acetate was inkjet printed to form patterned elastic microstructures, which are similar to microlens. The viscosity of diluted PDMS precursor mixtures is very stable and suitable for inkjet printing. The PDMS film produced from diluted inks exhibited lower elastic modulus and hardness values than non-diluted PDMS after cross-linking. The capacitor using printed PDMS as the microstructured dielectric layer has a high pressure sensitivity (10.4 kPa⁻¹ best) in the pressure range of 0–70 Pa, which dramatically drops to 0.43–0.52 kPa⁻¹ under an applied pressure in the range of 2–8 kPa. The printed PDMS based triboelectric sensors could be controlled to produce large voltage signals up to 1.23 V with damped vibrations and without any amplification. The mechanical properties, microstructure shape, and coverage play important roles in PDMS based devices. The directly inkjet printed PDMS dielectric layer with controlled mechanical properties and microstructures opens up the possibility of using the PDMS and its composites in functional electrical devices.

This work was supported by the project of the Science and Technology Program of Guangdong Province (2016B090906002), the Postdoctoral Foundation of Jiangsu Province (Grant No. 1501065C), and the National Natural Science Foundation of China (Grant Nos. 51603227, 51603228, and 51673214).

- ¹C. Liu, *Adv. Mater.* **19**(22), 3783–3790 (2007).
- ²A. P. Quist, E. Pavlovic, and S. Oscarsson, *Anal. Bioanal. Chem.* **381**(3), 591–600 (2005).
- ³S. Seethapathy and T. Gorecki, *Anal. Chim. Acta* **750**, 48–62 (2012).
- ⁴J. C. Lotters, W. Olthuis, P. H. Veltink, and P. Bergveld, *J. Micromech. Microeng.* **7**(3), 145–147 (1997).
- ⁵A. J. T. Teo, A. Mishra, I. Park, Y. J. Kim, W. T. Park, and Y. J. Yoon, *ACS Biomater. Sci. Eng.* **2**(4), 454–472 (2016).
- ⁶T. K. Shih, C. F. Chen, J. R. Ho, and F. T. Chuang, *Microelectron. Eng.* **83**(11–12), 2499–2503 (2006).
- ⁷S. H. Jang and H. M. Yin, *Appl. Phys. Lett.* **106**(14), 141903 (2015).
- ⁸G. Schwartz, B. C. K. Tee, J. G. Mei, A. L. Appleton, D. H. Kim, H. L. Wang, and Z. N. Bao, *Nat. Commun.* **4**(5), 1859 (2013).
- ⁹F. R. Fan, L. Lin, G. Zhu, W. Z. Wu, R. Zhang, and Z. L. Wang, *Nano Lett.* **12**(6), 3109–3114 (2012).
- ¹⁰J. H. Kim, B. K. Yun, J. H. Jung, and J. Y. Park, *Appl. Phys. Lett.* **108**(13), 133901 (2016).
- ¹¹S. C. B. Mannsfeld, B. C. K. Tee, R. M. Stoltenberg, C. V. H. H. Chen, S. Barman, B. V. O. Muir, A. N. Sokolov, C. Reese, and Z. N. Bao, *Nat. Mater.* **9**(10), 859–864 (2010).
- ¹²X. W. Wang, Y. Gu, Z. P. Xiong, Z. Cui, and T. Zhang, *Adv. Mater.* **26**(9), 1336–1342 (2014).
- ¹³Q. Hu, H. Wu, J. Sun, D. H. Yan, Y. L. Gao, and J. L. Yang, *Nanoscale* **8**, 5350–5357 (2016).
- ¹⁴C. J. Zhang, Q. Luo, H. Wu, H. Y. Li, J. Q. Lai, G. Q. Ji, L. P. Yan, X. F. Wang, D. Zhang, J. Lin, L. W. Chen, J. L. Yang, and C. Q. Ma, *Org. Electron.* **45**, 190–197 (2017).
- ¹⁵H. Wu, C. J. Zhang, K. X. Ding, L. J. Wang, Y. L. Gao, and J. L. Yang, *Org. Electron.* **45**, 302–307 (2017).
- ¹⁶H. Lu, J. Lin, N. Wu, S. H. Nie, Q. Luo, C. Q. Ma, and Z. Cui, *Appl. Phys. Lett.* **106**(9), 093302 (2015).
- ¹⁷Y. L. Sung, J. Jeang, C. H. Lee, and W. C. Shih, *J. Biomed. Opt.* **20**(4), 47005 (2015).
- ¹⁸A. L. Thangawng, R. S. Ruoff, M. A. Swartz, and M. R. Glucksberg, *Biomed. Microdevices* **9**(4), 587–595 (2007).
- ¹⁹K. Choonee, R. R. A. Syms, M. M. Ahmad, and H. Zou, *Sens. Actuators, A* **155**(2), 253–262 (2009).
- ²⁰T. R. E. Simpson, B. Parbhoo, and J. L. Keddie, *Polymer* **44**(17), 4829–4838 (2003).
- ²¹W. C. Oliver and G. M. Pharr, *J. Mater. Res.* **19**(1), 3–20 (2004).
- ²²Y. T. Hang, G. P. Liu, K. Huang, and W. Q. Jin, *J. Membr. Sci.* **494**, 205–215 (2015).
- ²³I. D. Johnston, D. K. McCluskey, C. K. L. Tan, and M. C. Tracey, *J. Micromech. Microeng.* **24**(3), 035017 (2014).